Recessive Mutations in *CFAP74* Cause Primary Ciliary Dyskinesia with Normal Ciliary Ultrastructure

To the Editor:

Motile cilia and sperm flagella are specialized hair-like organelles that share a common 9 + 2 microtubule-based axonemal ultrastructure of one central pair (CP) complex surrounded by nine peripheral doublets and numerous associated structures. Although in respiratory epithelial cells the coordinated ciliary beating enables mucociliary clearance of the airways, flagellar beating is essential for sperm cells to propel through the female reproductive tract for reproduction (1).

Mutations in numerous ciliary genes can lead to various degrees of ciliary and/or flagellar beating impairment, resulting in different but partially overlapping disease entities referred to as motile ciliopathies. Primary ciliary dyskinesia (PCD) is the hallmark motile ciliopathy, in which impaired mucociliary clearance ultimately leads to chronic destructive airway disease primarily characterized by localized bronchiectasis. Chronic upper respiratory tract symptoms include rhinitis and/or sinusitis and middle ear involvement. Further clinical manifestations of PCD can include situs abnormalities, reduced fertility, and/or rarely hydrocephalus (2). PCD is a rare disease, and various complex diagnostic steps are necessary to confirm the diagnosis. Genetic analysis can identify causative mutations in only about 70% of cases (3). Thus, gene discovery and adequate clinical phenotyping remains important to improve PCD diagnostics.

The term "multiple morphological abnormalities of the sperm flagella" (MMAF) was originally proposed for patients with asthenoteratozoospermia lacking any additional PCD specific respiratory symptoms (4). However, this distinction has become less clear. Mutations in *SPEF2*, which encodes a CP-associated protein, were originally described in males with MMAF but later demonstrated to cause a PCD phenotype (5–7). CP complex associated defects are difficult to identify because affected individuals present no situs abnormalities and show subtle changes in high-speed video microscopy analysis (HSVMA) (7). CFAP74 (cilia and flagella associated protein 74) is the mammalian homolog of FAP74, a subunit of the C1d projection of the central apparatus (Figure E5 in the data supplement) as demonstrated in *Chlamydomonas* (8). Flagella of *FAP74* knockdown *Chlamydomonas* show abnormal beating patterns with reduced frequencies (9). A recent study reported two patients with biallelic mutations in *CFAP74* that cause MMAF. Both patients also suffered from chronic airway disease; therefore, PCD was suspected but not assessed (10).

Here, we report three affected individuals from two families with compound heterozygous mutations in *CFAP74* and demonstrate abnormal ciliary beating and reduced mucociliary clearance responsible for the PCD phenotype. (Detailed methods description, clinical findings, and results are provided in the data supplement.) Two individuals were identified using a genetic panel that included *CFAP74*. Subsequently, genetic testing of one symptomatic sister was performed using Sanger sequencing. Three different novel loss-of-function mutations in *CFAP74* were identified (Figures 1A and 1B). OP-3882 II1 and OP-3882 II2 are siblings descended from a nonconsanguineous German family. Both were identified with c.907del, p.Gln303LysfsTer65 and c.4380_4381dup, p.Phe1461SerfsTer12 mutations in *CFAP74*. In OP-4027 II1, the *CFAP74* mutation c.4380_4381dup and also the mutation c.1706dup, p.Gly570TrpfsTer10 were identified. Segregation analysis of the parents confirmed compound heterozygosity in all cases. The absence of CFAP74 in *CFAP74*-mutant respiratory epithelial cells was demonstrated by immunoblot analysis of axonemal extracts using anti-CFAP74 antibodies confirming recessive loss-of-function mutations in OP-3882 II1 and OP-3882 II2 (Figures 1C–1E).

All three *CFAP74*-affected individuals have normal situs composition (*situs solitus*). Medical histories reported recurrent respiratory infections of various degrees since early childhood. Lung function testing gave normal results or minor alterations in all individuals. Exemplary evidence of upper and lower airway disease in form of localized bronchiectasis, polyposis nasi, and pansinusitis is demonstrated in Figures 2A and 2B. Remarkably, nasal NO production rates were in the normal range, well over the currently established cutoff value for PCD diagnosis (11). OP-3882 II1 was diagnosed with oligoasthenospermia, and most sperm cells presented a mosaic of MMAF including short, coiled, bent, absent, or irregular wide flagella (Figure E1).

Transmission electron microscopy (TEM) of respiratory cilia of two affected subjects proved a regular ciliary ultrastructure (Figure E2). Consistent with this, high-resolution immunofluorescence microscopy of respiratory epithelial cells from all affected showed a normal localization of the outer dynein arms, nexin-dynein regulatory complexes, and the CP-associated protein SPEF2 (Figures E3 and E4). HSVMA of *CFAP74*-mutant human respiratory epithelial cells showed reduced ciliary beat frequencies (Figure E6). Subtle abnormalities of the ciliary beating pattern (CBP) were identified. CBP was mostly coordinated but showed a slightly reduced beating amplitude with a partially stiff as well as rotatory pattern (Videos E01–E04).

Particle transport analyses of air–liquid interface cultured respiratory epithelial cells showed a nondirected transport and a significantly reduced particle transport velocity in both *CFAP74*-mutant individuals (Figures 2C and E7 and Videos E09–E10). Mutant respiratory epithelial cells were unable to generate a

Supported by grants from the Deutsche Forschungsgemeinschaft (DFG OM6/7, OM6/8, OM6/10, OM6/14, OM6/16, and CRU 326 [subprojects OM6/11 (H. Omran), RA3522/1-1 (J.R.), OL 450/1 (H. Olbrich), and HJ 7/1-1 (R.H.)]), the Interdisziplinäres Zentrum für Klinische Forschung (IZKF), Medizinische Fakultät, Westfälische Wilhelms-Universität Münster (Om2/009/12, Om2/015/16, and Om2/010/20), and the European Commission Registry Warehouse (Horizon2020 GA 777295) and BESTCILIA EU FP7 GA 305404. This work is generated within the European Reference Network for rare respiratory diseases ERN-LUNG.

This letter has a data supplement, which is accessible from this issue's table of contents at www.atsjournals.org.

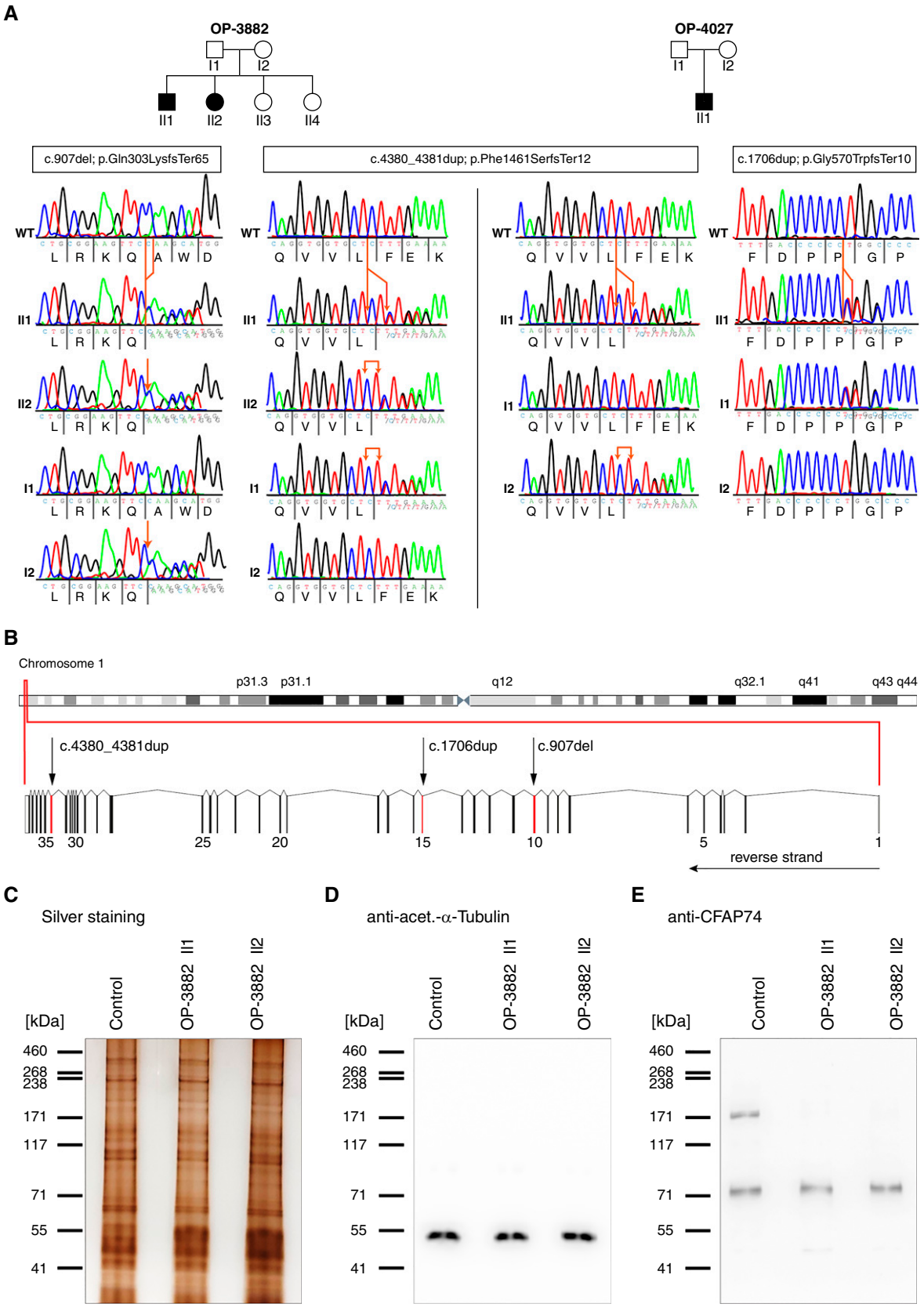

Figure 1. Compound heterozygous loss-of-function mutations in *CFAP74* in OP-3882 II1, OP-3882 II2 and OP-4027 II1 cause PCD. (*A*) Pedigrees of the two index families are shown. Electropherograms of Sanger sequencing results of *CFAP74* amplicons of individuals

directed fluid flow across the epithelial surface. This finding provides proof of a decreased ciliary clearance capacity consistent with chronic airway disease present in the *CFAP74*-mutant individuals.

In conclusion, we demonstrate that the CP apparatus-associated protein CFAP74 not only plays an important role for sperm architecture and function but is also important for the integrity of ciliary motility in respiratory epithelial cells and for sustaining ciliary clearance in the airways. Mutations of *CFAP74* result in defects of the CP, explaining the observed subtle CBP abnormalities. We reported similar subtle beating abnormalities in individuals carrying pathogenic mutations in genes encoding other CP associated proteins such as HYDIN and SPEF2 (7, 12). Like individuals with *HYDIN* and *SPEF2* mutations, all individuals with *CFAP74* mutations display no laterality defects, which is consistent with findings in the corresponding mouse models. In all mouse models for CP defects, no situs abnormalities have been reported, but they showed airway disease consistent with PCD (13). The lack of laterality defects in *CFAP74* mutations makes it even more difficult to consider an underlying PCD diagnosis.

Common diagnostic algorithms might not have detected PCD in the reported patients. Evidence-based guidelines were published by the European Respiratory Society in 2017 and the American Thoracic Society in 2018, respectively (14, 15). Nasal NO measurement is relevant both in the European Respiratory Society and American Thoracic Society PCD diagnostic guidelines (14, 15). Even though it is known that normal nasal NO values cannot rule out PCD diagnosis (16), nasal NO testing is still widely used as a screening tool, leaving the risk of abandoning the diagnostic process prematurely. The same applies to the analysis of ciliary ultrastructure using TEM, where the diagnostic gap is aggravated as normal nasal NO can coincide with normal TEM (16, 17). We found normal NO values and slightly reduced ciliary beat frequencies with subtle beating abnormalities and normal 9 + 2 ultrastructure in the affected individuals. We also checked whether the axonemal localization of the CP-associated protein SPEF2 is altered in *CFAP74*-mutant respiratory cilia (Figure E4). However, we found no abnormalities, which is probably explained by the localization of SPEF2 to the C1b projection and CFAP74 to the C1d projection, respectively (Figure E5). Thus, without genetic testing and additional assays such as HSVMA and particle transport analyses, establishing a PCD diagnosis in such cases is challenging.

Taken together, we demonstrate that pathogenic mutations in *CFAP74* cause PCD with normal situs and contribute to the genetic and clinical diagnosis of PCD with normal nasal NO production rates, normal ciliary ultrastructure, and subtle ciliary beating defects. This highlights the importance of genetic testing as well as establishing new functional analyses like particle-tracking experiments (Figure 2C) in the diagnostic process (18). We conclude that regular screening for *CFAP74* mutations should be included for the genetic workup of individuals suspected to suffer from PCD.

This study was conducted according to the guidelines of the Declaration of Helsinki and approved by the Ethics Committee of the Westphalian Wilhelms University of Muenster (2015-104-f-S). Informed consent was obtained from all subjects involved in the study. ■

Figure 1. (*Continued*). OP-3882 II1 and OP-3882 II2 demonstrate a heterozygous deletion of one base pair (*CFAP74* c.907del) and on the second allele, a duplication of two base pairs (*CFAP74* c.4380_4381dup) both predicting a premature termination of translation (p.Gln303LysfsTer65 and p.Phe1461SerfsTer12) (red arrow; amino acids are indicated below nucleotide sequence). The wild-type (WT) sequence is shown in the top row. Individual OP-3882 I1 carries only the duplication in a heterozygous state, confirming segregation. Sequencing chromatograms of *CFAP74* amplicons of individuals OP-4027 II1 demonstrate the same duplication of two base pairs (*CFAP74* c.4380_4381dup) predicting a premature termination of translation (p.Phe1461SerfsTer12) and an additional heterozygous duplication of one base pair (*CFAP74* c.1706dup) resulting in a premature termination of translation (p.Gly570TrpfsTer10 (red arrow; amino acids are indicated below nucleotide sequence). The WT sequence is shown in the top row. The parents OP-4027 I1 and OP-4027 I2 carry only one of the two mutations, respectively, in a heterozygous state, confirming segregation. (*B*) Schematic presentation of *CFAP74* on chromosome 1 is shown along with the transcript diagram. The positions of the identified mutations are indicated by exons highlighted in red. (*C–E*) Immunoblot analysis demonstrates the absence of the CFAP74 protein (full-length ~179 kDa isoform, Q9C0B2) in *CFAP74*-mutant respiratory epithelial cells. Axonemal extracts from *CFAP74*-mutant and control human primary respiratory epithelial cells were prepared from air–liquid interface (ALI) cultured respiratory cells. (*C*) Silver staining after lithium dodecyl sulfate-PAGE of normalized amounts of loaded protein (2 μg per sample) demonstrates the integrity of protein recovery from the axonemal preparations. (*D*) Immunoblot using anti-acetylated-α-tubulin (50 kDa) antibodies also confirmed equal amounts of axonemal proteins. (*E*) Immunoblot analysis of healthy control axonemal extracts and *CFAP74*-mutant axonemal extracts was performed with rabbit polyclonal anti-CFAP74 antibodies. Two bands were detectable in axonemal extracts from a healthy control subject. The higher molecular weight band corresponds to the predicted protein size of the large CFAP74 isoform (179 kDa). This band was absent in both *CFAP74*-mutant axonemal extracts consistent with loss-of function mutations. Only one band at a predicted size around 100 kDa remained detectable, which probably represents unspecific binding or a shorter CFAP74 isoform.

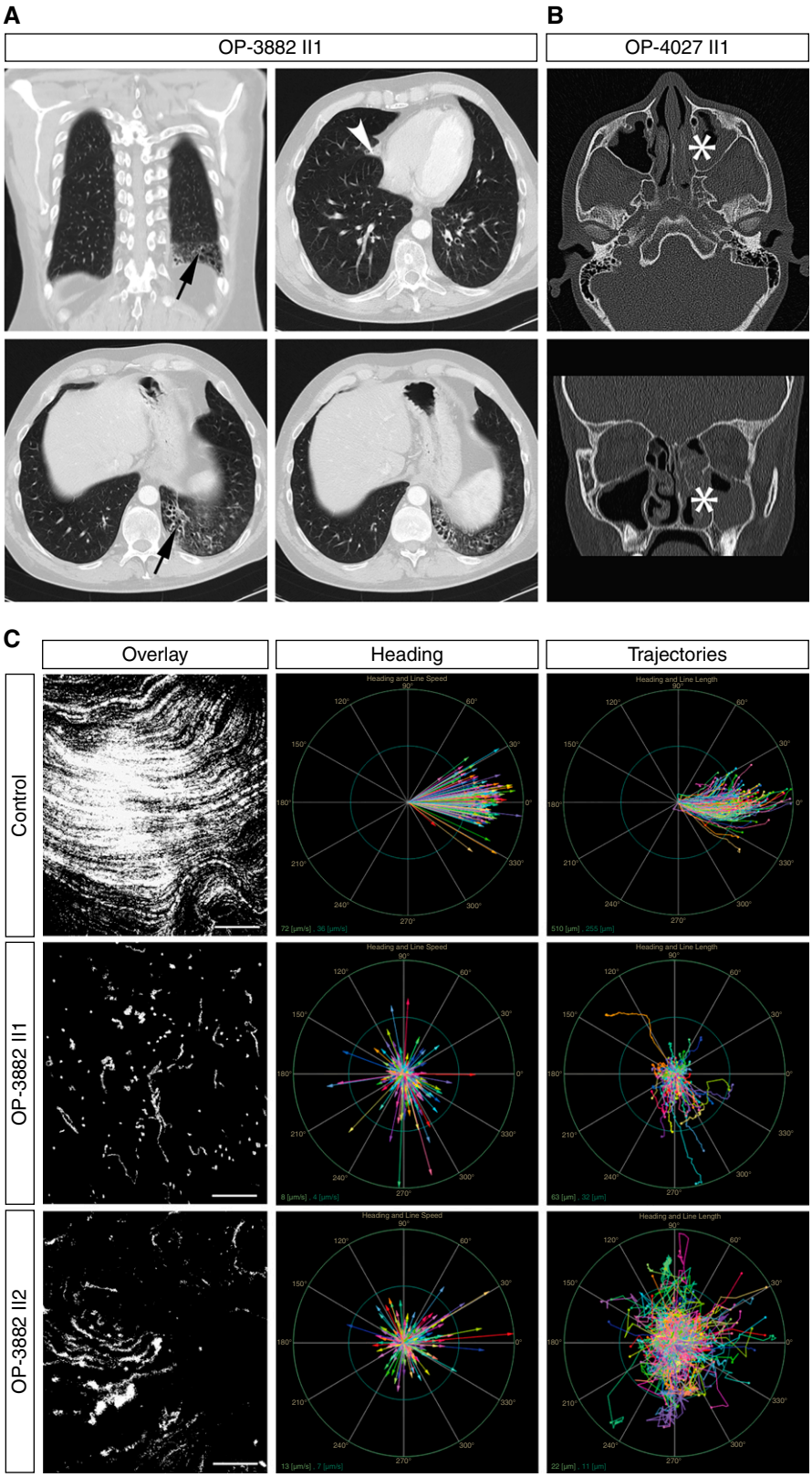

Figure 2. *CFAP74* mutations lead to chronic airway disease caused by impaired ciliary airway clearance. (*A*) Computed tomography scans of the lungs show localized bronchiectasis of the left lower lobe (indicated by black arrows) and dystelectasis of the right middle lobe in OP-3882 II1 (white arrowhead). (*B*) Images of the paranasal sinus of OP-4027 II1 show polyposis consistent with chronic sinusitis (indicated by asterisks). (*C*) Functional analyses of the ciliary beating of respiratory cells of a healthy control and two *CFAP74*-mutant individuals. Tracking experiments

Author disclosures are available with the text of this letter at www.atsjournals.org.

Acknowledgment: The authors thank the PCD individuals and their families for participation and all referring physicians. They acknowledge the German PCD support group "Kartagener Syndrom und Primäre Ciliäre Dyskinesie e.V.". They thank Andreas Borgscheiper, Simone Helms, Martina Herting, Laura Schwiddessen, Sironi Sivalingam, and Kai Wohlgemuth for providing excellent technical assistance.

Luisa Biebach, M.D.*
Sandra Cindrić, Ph.D.*
Julia Koenig, M.Sc.
Isabella Aprea, M.Sc.
Gerard W. Dougherty, Ph.D.
Johanna Raidt, M.D.
Diana Bracht, Ph.D.
University Children's Hospital Muenster
Muenster, Germany

Renate Ruppel, M.D.
University Hospital Erlangen
Erlangen, Germany

Jens Schreiber, M.D.
Otto-von-Guericke-University
Magdeburg, Germany

Rim Hjeij, Ph.D.
Heike Olbrich, Ph.D.
Heymut Omran, M.D.‡
University Children's Hospital Muenster
Muenster, Germany

ORCID IDs: 0000-0003-2863-4841 (L.B.); 0000-0002-8303-100X (S.C.); 0000-0001-5681-874X (I.A.); 0000-0001-6905-8110 (G.W.D.); 0000-0002-1571-2647 (J.R.); 0000-0002-2151-038X (D.B.); 0000-0001-6795-2282 (J.S.); 0000-0003-1464-7289 (R.H.); 0000-0003-4355-353X (H. Olbrich); 0000-0003-0282-6765 (H. Omran).

*These authors contributed equally to this work.
‡Corresponding author (e-mail: heymut.omran@ukmuenster.de).

References

1. Wallmeier J, Nielsen KG, Kuehni CE, Lucas JS, Leigh MW, Zariwala MA, *et al.* Motile ciliopathies. *Nat Rev Dis Primers* 2020;6:77.
2. Goutaki M, Meier AB, Halbeisen FS, Lucas JS, Dell SD, Maurer E, *et al.* Clinical manifestations in primary ciliary dyskinesia: systematic review and meta-analysis. *Eur Respir J* 2016;48:1081–1095.
3. Horani A, Ferkol TW. Advances in the genetics of primary ciliary dyskinesia: clinical implications. *Chest* 2018;154:645–652.
4. Ben Khelifa M, Coutton C, Zouari R, Karaouzène T, Rendu J, Bidart M, *et al.* Mutations in DNAH1, which encodes an inner arm heavy chain dynein, lead to male infertility from multiple morphological abnormalities of the sperm flagella. *Am J Hum Genet* 2014;94:95–104.
5. Tu C, Nie H, Meng L, Wang W, Li H, Yuan S, *et al.* Novel mutations in SPEF2 causing different defects between flagella and cilia bridge: the phenotypic link between MMAF and PCD. *Hum Genet* 2020;139:257–271.
6. Liu W, Sha Y, Li Y, Mei L, Lin S, Huang X, *et al.* Loss-of-function mutations in SPEF2 cause multiple morphological abnormalities of the sperm flagella (MMAF). *J Med Genet* 2019;56:678–684.
7. Cindrić S, Dougherty GW, Olbrich H, Hjeij R, Loges NT, Amirav I, *et al.* *SPEF2*- and *HYDIN*- mutant cilia lack the central pair-associated protein SPEF2, aiding primary ciliary dyskinesia diagnostics. *Am J Respir Cell Mol Biol* 2020;62:382–396.
8. Samsel Z, Sekretarska J, Osinka A, Wloga D, Joachimiak E. Central apparatus, the molecular kickstarter of ciliary and flagellar nanomachines. *Int J Mol Sci* 2021;22:1–22.
9. DiPetrillo CG, Smith EF. Pcdp1 is a central apparatus protein that binds Ca(2+)-calmodulin and regulates ciliary motility. *J Cell Biol* 2010;189: 601–612.
10. Sha Y, Wei X, Ding L, Ji Z, Mei L, Huang X, *et al.* Biallelic mutations of CFAP74 may cause human primary ciliary dyskinesia and MMAF phenotype. *J Hum Genet* 2020;65:961–969.
11. Leigh MW, Hazucha MJ, Chawla KK, Baker BR, Shapiro AJ, Brown DE, *et al.* Standardizing nasal nitric oxide measurement as a test for primary ciliary dyskinesia. *Ann Am Thorac Soc* 2013;10: 574–581.
12. Olbrich H, Schmidts M, Werner C, Onoufriadis A, Loges NT, Raidt J, *et al.*; UK10K Consortium. Recessive HYDIN mutations cause primary ciliary dyskinesia without randomization of left-right body asymmetry. *Am J Hum Genet* 2012;91:672–684.
13. Sironen A, Kotaja N, Mulhern H, Wyatt TA, Sisson JH, Pavlik JA, *et al.* Loss of SPEF2 function in mice results in spermatogenesis defects and primary ciliary dyskinesia. *Biol Reprod* 2011;85:690–701.
14. Lucas JS, Barbato A, Collins SA, Goutaki M, Behan L, Caudri D, *et al.* European Respiratory Society guidelines for the diagnosis of primary ciliary dyskinesia. *Eur Respir J* 2017; 49:1601090.
15. Shapiro AJ, Davis SD, Polineni D, Manion M, Rosenfeld M, Dell SD, *et al.*; American Thoracic Society Assembly on Pediatrics. Diagnosis of primary ciliary dyskinesia: an official American thoracic society clinical practice guideline. *Am J Respir Crit Care Med* 2018; 197:e24–e39.
16. Shapiro AJ, Davis SD, Leigh MW, Knowles MR, Lavergne V, Ferkol T. Limitations of nasal nitric oxide testing in primary ciliary dyskinesia. *Am J Respir Crit Care Med* 2020;202:476–477.
17. Shapiro AJ, Leigh MW. Value of transmission electron microscopy for primary ciliary dyskinesia diagnosis in the era of molecular medicine: genetic defects with normal and non-diagnostic ciliary ultrastructure. *Ultrastruct Pathol* 2017;41:373–385.
18. Wallmeier J, Frank D, Shoemark A, Nöthe-Menchen T, Cindric S, Olbrich H, *et al.* de novo mutations in FOXJ1 result in a motile ciliopathy with hydrocephalus and randomization of left/right body asymmetry. *Am J Hum Genet* 2019;105:1030–1039.

Figure 2. (*Continued*). were performed with fully differentiated respiratory epithelial cells cultured under ALI conditions. Fluorescent beads were added to the apical compartment of the ALI-filter and recorded. Corresponding differential interference contrast videos were taken to record cell morphology and ciliary beating. A highly nondirected particle transport was observed in all analyzed cultures from both *CFAP74*-mutant individuals. Visualization of the ciliary clearance (particle transport) by means of overlay of the acquired images and direction diagram as vector (heading) and path representation (trajectories). Scale bars, 100 μm. In the vector representation, the direction of each object is represented as a colored arrow, where the length of the arrow corresponds to the respective object velocity. In the path representation, a path corresponds to the real object movements. The length of the paths corresponds to the respective path length.